Nanomotors

Deutsche Ausgabe: DOI: 10.1002/ange.201607330
Internationale Ausgabe: DOI: 10.1002/anie.201607330

Synthesis of Chemically Asymmetric Silica Nanobottles and Their Application for Cargo Loading and as Nanoreactors and Nanomotors

*Deliang Yi, Qian Zhang, Yinghua Liu, Jiaying Song, Yi Tang, Frank Caruso, and Yajun Wang**

Abstract: *We report the synthesis of chemically asymmetric silica nanobottles (NBs) with a hydrophobic exterior surface (capped with 3-chloropropyl groups) and a hydrophilic interior surface for spatially selective cargo loading, and for application as nanoreactors and nanomotors. The silica NBs, which have a "flask bottle" shape with an average diameter of 350 nm and an opening of ca. 100 nm, are prepared by anisotropic sol–gel growth in a water/n-pentanol emulsion. Due to their chemically asymmetric properties, nanoparticles (NPs) with hydrophilic or hydrophobic surface properties can be selectively loaded inside the NBs or on the outside of the NBs, respectively. A high-performance nanomotor is constructed by selectively loading catalytically active hydrophilic Pt NPs inside the NBs. It is also demonstrated that these NBs can be used as vessels for various reactions, such as the in situ synthesis of Au NPs, and using Au NP-loaded NBs as nanoreactors for catalytic reactions.*

Janus particles with various morphologies and surface properties have gained increasing interest since they were described by de Gennes in 1992.[1] Due to their chemical asymmetry,[2] Janus particles have been widely applied in a range of applications, such as superstructure assembly,[3] solid surfactants,[4] self-propelled nanomotors,[5] drug delivery,[6] and clinical diagnosis.[7] Among them, self-propelled nanomotors are small autonomous devices capable of performing complex tasks in fluids. These autonomous devices have the potential to play key roles in cargo transport, biosensing, environmental science, and microsurgery.[8,9] To date, various methods have been reported for the construction of nanomotors with different structures, such as electrochemical deposition to prepare bimetallic nanomotors,[10] a template-based approach to fabricate conical tubular micromotors,[8a,11] rolling up strain engineered inorganic nanomembranes to prepare tubular nanomotors,[12] and the dynamic shadowing growth method to fabricate heterogeneous self-motile structures.[13] However, these methods require specialized equipment or complicated experimental procedures that can be difficult to scale up.

Herein, we report the one-pot preparation of silica hollow particles with a flask bottle shape (denoted as silica nanobottles, NBs) that possess a hydrophobic exterior surface and a hydrophilic interior. We also demonstrate a simple and efficient method to prepare nanomotors through specific loading of Pt nanoparticles (NPs) inside the chemically asymmetric NBs. The silica NBs have a unique structure comprising a large cavity and a narrow opening, which connects the cavity with the outer environment. Generating hollow particles with large voids in the shells, such as bottle, stomatocyte and bowl-like nanoarchitectures, has attracted interest for effective diffusion and high uptake capacity of relatively big guest molecules and nanoparticles.[14] Due to their unique surface chemical properties, the chemically asymmetric silica NBs reported here can be used to selectively carry cargo into their cavities in solution based on the interactions between the cargo and NB interior surface.

The synthesis of the chemically asymmetric silica NBs is inspired by our recent work on synthesizing hydrophobic silica nanowires,[15] which were anisotropically grown in a water/oil emulsion system.[16] Our current work uses (3-chloropropyl)trimethoxysilane (CPTMS) with a mildly hydrophobic 3-chloropropyl group instead of the highly hydrophobic trimethoxy(octadecyl)silane (OTMS) previously used to prepare the high aspect ratio nanowires. The formation of the NBs involved arranging hydrolyzed CPTMS molecules at the water–oil interface, and the anisotropic deposition of hydrolyzed tetrabutylorthosilicate (TBOS) inside the arranged CPTMS layer to form a thin silica shell. By expanding the silica shell, aqueous solution was gradually extruded out of the droplet to form the bottle neck and opening of the NBs.

A postulated growth mechanism for synthesizing such chemically asymmetric silica NBs is illustrated in Figure 1 a–c. The CPTMS molecules hydrolyze when they meet the water droplets in basic conditions. As the hydrolyzed CPTMS molecules are amphiphilic, its hydrophilic $-Si(-O^-)_3$ component will insert into the water droplet while the hydrophobic chloropropyl tail remains in the *n*-pentanol, thus forming a thin silica film at the droplet surface (Figure 1 a). TBOS hydrolyzes when it migrates from the oil phase into the water phase, and condensates at the aforementioned silica film to form "bowl-like" silica with a thicker shell (Figure S1a). With the co-condensation of hydrolyzed CPTMS and TBOS, the "bowl-like" silica was drawn into the hollow silica shell (Figure 1 b and Figure S1b in the Supporting Information). The continuous deposition of hydrolyzed TBOS in the shell from the water side extruded the water and produced a new

[*] Dr. D. L. Yi, Q. Zhang, Y. H. Liu, J. Y. Song, Prof. Y. Tang, Prof. Y. J. Wang
Department of Chemistry, Fudan University
Shanghai 200433 (P.R. China)
E-mail: yajunwang@fudan.edu.cn
Prof. F. Caruso
ARC Centre of Excellence in Convergent Bio-Nano Science and Technology, and the Department of Chemical and Biomolecular Engineering, The University of Melbourne
Parkville, Victoria 3010 (Australia)
Supporting information and the ORCID identification number(s) for the author(s) of this article can be found under http://dx.doi.org/10.1002/anie.201607330.

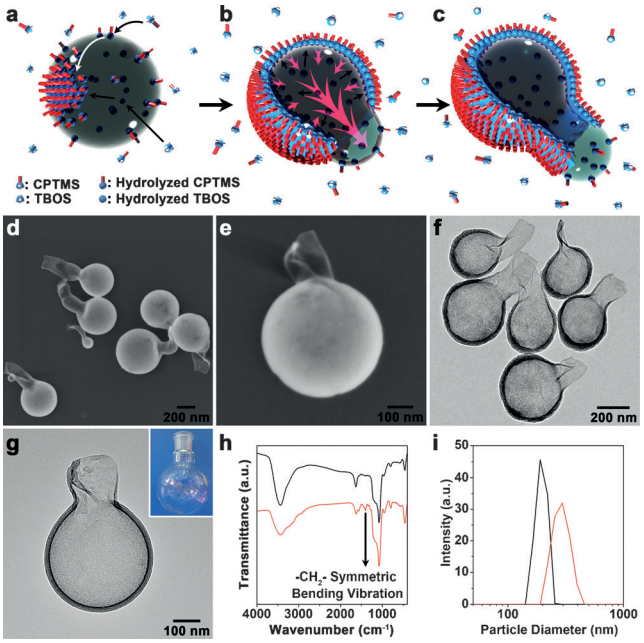

Figure 1. a–c) Illustration of the formation of chemically asymmetric silica NBs. a) Hydrolyzed CPTMS arranged at the water–oil interface with hydrolyzed TBOS condensed at the interface from the water side. b) The formation of a hybrid silica shell from the co-condensation of CPTMS and TBOS; the continuous deposition of TBOS extrudes water out of the shell to form a new water-oil interface. c) The co-condensation of CPTMS and TBOS at the newly formed water-oil interface caused the formation of chemically asymmetric NBs. d, e) SEM images and f, g) TEM images of the silica NBs. h) FTIR spectra of the NBs before (red line) and after (black line) removal of organic residues. i) DLS measurement of particle size distribution of the as-prepared NBs (black line) and NBs after removal of the hydrophobic capping organic groups (red line).

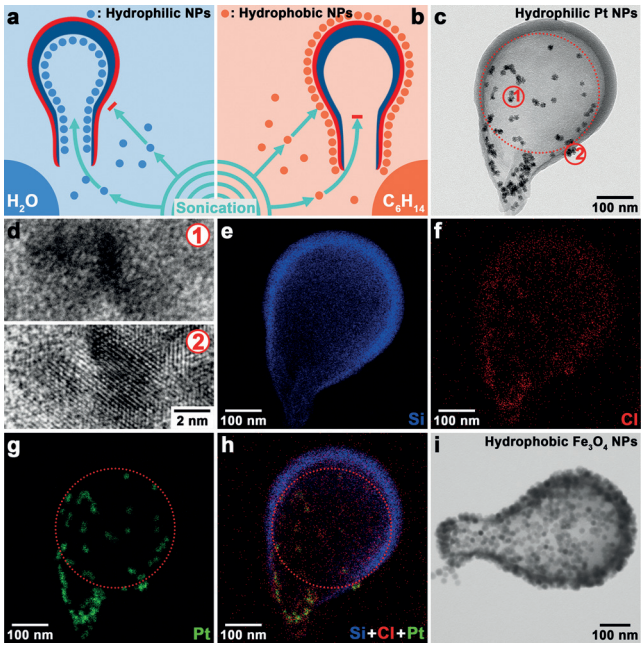

Figure 2. a, b) Selective loading of hydrophilic NPs on the interior surface, and hydrophobic NPs on the exterior surface of the chemically asymmetric silica NBs. c) TEM image of hydrophilic Pt NPs loaded in the cavity of the silica NBs. d) High-resolution TEM images of Pt NPs loaded inside the NBs (1) and adsorbed on the outer surface of the NBs (2). e–h) Elemental mapping profiles of the Pt NPs@NBs shown in (c). i) TEM image of hydrophobic Fe_3O_4 NPs adsorbed on the hydrophobic exterior surface of the NBs.

oil–water interface. The co-condensation at the newly formed water–oil interface caused the silica to form into a flask bottle-like structure with an opening (Figure 1 c). The synthesized silica particle resembles a flask bottle shape, and has an average diameter of 350 ± 70 nm and a neck diameter of about 120 nm (Figure 1 d–g). The thickness of the silica shell is about 10 nm at the body of the bottle, gradually decreasing at the bottle neck, which has a channel of ca. 100 nm in diameter connecting the inner cavity of the NBs to the environment. The shell thickness of the NBs increased when using siloxane (e.g., tetraethyl orthosilicate, TEOS) with a higher hydrolysis rate, and the particle shape developed a tube-like structure by using OTMS with higher hydrophobicity (Figure S2).

Capping of the exterior surface of the NBs with organic 3-chloropropyl groups is demonstrated from the elemental mapping data (Figure 2 f, Figure S3c) and the symmetric bending vibrations of $-CH_2-$ (1400 and 1425 cm^{-1}) in the Fourier transform infrared (FTIR) spectra (Figure 1 h). Dynamic light scattering (DLS) revealed that the silica NBs had a particle size distribution (PSD) of 150–250 nm (Figure 1 i), smaller than the particle size observed from the scanning electron microscopy (SEM) and transmission electron microscopy (TEM) images (Figure 1 d–g). The smaller size obtained from DLS measurements is likely caused by the capped 3-chloropropyl groups on the particle surface, as previous studies revealed that hydrophobic coatings on nanoparticles can significantly decrease the interaction between water and nanoparticles, thereby reducing their hydrodynamic diameters.[17] Interestingly, the PSD of the silica NBs increased to 200–450 nm after removal of the 3-chloropropyl groups by Piranha solution (Figure 1 i, Figure S3d), which is consistent with the particle size measured from TEM and SEM images (Figure 1 d–g).

As the silica NBs possess a hydrophobic exterior surface and a hydrophilic interior surface, selective loading of cargo with different surface properties in the NBs is feasible via amphiphilic interaction (Figure 2 a,b). For example, citrate-capped hydrophilic NPs (e.g., Pt and Fe_3O_4 NPs) can be loaded inside the NBs when the NPs were sonicated with Janus silica NBs in water (Figure 2 c, Figure S4a). TEM images show that most of the hydrophilic Pt NPs were loaded inside the NBs (Figure 2 c). The crystal lattice of the Pt NPs can be clearly distinguished for NPs located outside the NBs, but less so for NPs loaded inside the NBs, largely due to electron blocking of the siliceous NB shell (Figure 2 d).[18] Elemental mapping profiles (Figure 2 e–h) reveal that the Pt NPs located at the bottom of the NBs (inside the red circle) were less bright than Pt NPs loaded at the neck and outer surface (outside the red circle). This is likely because the silica shell at the base of the NBs is thicker than at the neck, which blocks more signal when analyzed by energy-dispersive X-ray spectroscopy. These results demonstrate that hydrophilic Pt

NPs can be efficiently loaded inside the chemically asymmetric NBs through hydrogen bonding between the silicon hydroxyl groups (interior surface of the NBs) and the carboxyl groups on the citrate-capped Pt NPs.[19] Further, the hydrophobic exterior surface of the NB weakened its interaction with water media and the hydrophilic NPs dispersed in water. Conversely, hydrophobic NPs (e.g., oleic acid-capped Fe_3O_4 NPs, dodecylamine-capped Pt NPs) were adsorbed on the exterior surface of the NBs in *n*-hexane due to hydrophobic forces (Figure 2i, Figures S4b, S5a). The Fe_3O_4 NPs-loaded NBs were collected in less than 5 s using a magnet (Figure S6), hence they potentially can be used in magnetic separation or for the magnetic-guided targeted delivery of NBs. As a control, the hydrophobic Fe_3O_4 NPs barely adhered on the NBs after the 3-chloropropyl-capping groups were removed from the exterior surface (Figure S5b).

The Pt NPs-loaded NBs resemble previously reported Pt NPs-loaded polymer stomatocytes with a bowl-shaped structure.[14c] Pt NPs loaded inside the NBs catalyzed the decomposition of H_2O_2 into O_2 and H_2O. The local concentration gradient of the O_2 caused its ejection from the NBs via the narrow opening,[14c] thereafter propelling Pt NPs@NBs forward (Figure 3a). Optical microscopy was used to observe

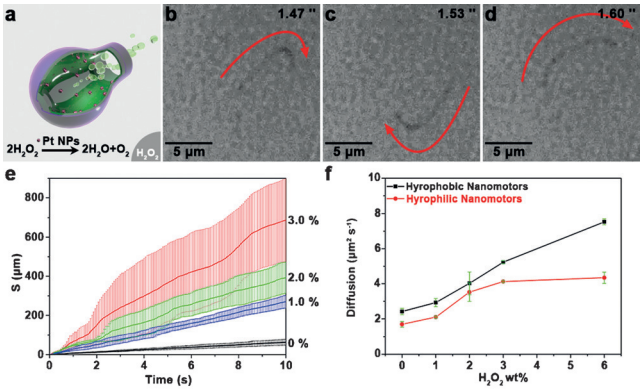

Figure 3. a) Self-propelling Pt NPs@NBs. b–d) Snapshots extracted from optical video of the chemically asymmetric silica nanomotor in 3.0 wt% H_2O_2 (The red arrows in (b)–(d) indicate the direction of movement of the nanomotor). e) Total distance travelled by the nanomotor in the presence of different concentrations of H_2O_2. f) The apparent diffusion coefficient of the nanomotors with (black) or without (red) hydrophobic organic groups on the exterior surface of the nanomotor. Six NBs were studied in each experiment condition in (e) and (f).

and record the motion of Pt NPs@NBs using H_2O_2 as a propellant. Pt NPs@NBs showed a typical "random walk" movement in pure H_2O (Movie S1). The velocity and orientation movement increased with the higher H_2O_2 concentrations (Movies S2 and S3). A circular motion was observed when the H_2O_2 concentration was increased to 3 wt.% (Movie S3). This is in good agreement with the previous report and theoretical modeling that tubular micromotors change dynamics to circular trajectories upon increasing the speed.[20] Figure 3b–d illustrates the trajectory of the nanomotor (extracted from the Movie S3). The nanomotor velocity was measured from the distance travelled by the Pt NPs@NBs in each frame of the recorded movies.[21] The trajectory was measured from its position in adjacent frames (Figure S7). The mean velocity of the nanomotors in H_2O was about $6.3 \pm 1.5\ \mu m\,s^{-1}$ (Figure S8); this was calculated by measuring the total distance travelled over 10 s. As expected, the velocity of the Pt NPs@NBs nanomotors increased with higher concentrations of H_2O_2, increasing to $68.8 \pm 21.3\ \mu m\,s^{-1}$ with the addition of 3.0 wt% H_2O_2. The total distance travelled by the nanomotors increased 10-fold when the H_2O_2 concentration increased from 0 to 3.0 wt% (Figure 3e).

The apparent diffusion coefficient of the nanomotor motion was measured by DLS, according to the size dependence of Brownian motion given by the Stokes–Einstein equation.[6b] The apparent diffusion coefficient increased from 2.4 to 7.5 $\mu m^2\,s^{-1}$ when the H_2O_2 concentration increased from 0 to 6.0 wt% (Figure 3f). To investigate the influence of surface properties of the nanomotor on its motion, the exterior chloropropyl groups were removed from the Pt NPs@NBs to obtain a hydrophilic surface. Although the apparent diffusion coefficient of the hydrophilic nanomotor increased as the H_2O_2 concentration increased, the value is lower than that obtained from the chemically asymmetric nanomotor and reached its limit of ca. 4 $\mu m^2\,s^{-1}$ at a H_2O_2 concentration of 3.0 wt% (Figure 3f). The diffusion coefficient of chemically asymmetric nanomotors was approximately two-fold higher than that of hydrophilic NB motors in the presence of 6.0 wt% H_2O_2. This can be attributed to the hydrophobic coating on the exterior surface of the nanomotor weakening the interaction with the surrounding solution; this would reduce the fluid drag and sliding friction,[22] thereby improving the motion of the nanomotors.[23] The influence is more significant when the NB motor moves at higher speed (Figure 3f), most likely due to the fluid drag of a nanoparticle being second order with respect to its velocity in static fluid. In addition to various strategies, such as changing composition[24] or geometry (e.g., from cylindrical to rocket shape)[8a,11] which can be exploited to improve nanomotor motion performance, capping NBs with a hydrophobic exterior surface provides a facile approach to improving the motion performance of nanomotors.

As the silica NBs have a hydrophilic interior surface and a large cavity connected to the environment through an opening, the cavity of the NBs can be efficiently used as a nanovessel for reactions in an aqueous environment. Chemically asymmetric NBs can be further applied as nanovessels for various reactions, such as NP preparation and molecular catalysis. Here, the in situ preparation of Au NPs is used as an example (Figure 4a–c). The NBs were filled with reactants (2.5×10^{-3} M chloroauric acid and 5×10^{-3} M sodium citrate) and the excess solution was removed through centrifugation in a Millipore ultrafiltration centrifuge tube. The color of the NBs gradually changed from white to dark purple in 30 min, indicating the formation of Au NPs. TEM characterization showed Au NPs with an average particle size of 10 nm were produced inside the NBs (Figure 4d), and no Au NPs were observed outside the NBs. This contributes to the chemically asymmetric properties of the NBs, as the

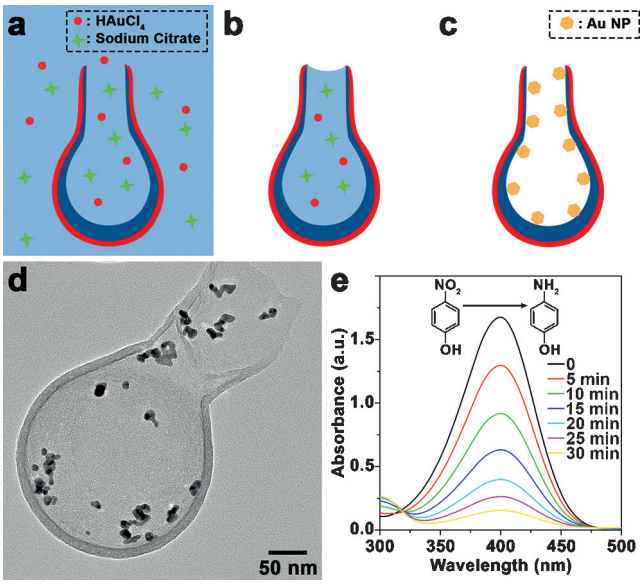

Figure 4. Chemically asymmetric silica NBs used as nanoreactors. a–c) Illustration of the in situ preparation of Au NPs in the chemically asymmetric NBs. a) Dispersion of silica NBs in a solution containing $HAuCl_4$ and sodium citrate. b) Removal of the excess solution by centrifugation with a Millipore centrifuge tube. c) Reduction of $HAuCl_4$ to Au NPs in 24 h. d) TEM image of Au NPs in situ prepared in the chemically asymmetric NBs. e) UV/Vis spectra of 4-nitrophenol catalytically reduced by Au NPs@NBs nanoreactors.

aqueous solution outside the NBs was efficiently removed due to its low attraction to the hydrophobic exterior surface. Meanwhile, the solution in the NBs remained inside during separation via centrifugation, largely due to the affinity between the hydrophilic interior surface and the capillary forces. Nucleation of the Au NPs was initiated automatically in the NBs by the reduction of $HAuCl_4$ with sodium citrate. The Au NP content in the NBs is 2.4 wt%, as measured by inductively coupled plasma atomic emission spectroscopy. The size of the Au NPs was limited to around 10 nm since the $HAuCl_4$ amount inside the NBs was fixed. To evaluate the catalytic performance of the Au NPs@NBs, a catalytic reduction of 4-nitrophenol was performed. The absorbance at 400 nm decreased with time (Figure 4e), indicating the reduction of 4-NP. The reduction of 4-NP catalyzed by Au NPs@NBs can be considered as a pseudo-first-order reaction with an apparent rate constant (k_{app}) of 0.08 min^{-1}. The relative rate constant was calculated to be 0.36 $s^{-1}mmol^{-1}$, which is comparable to previously reported Au NP-based nanoreactors (0.02–0.62 $s^{-1}mmol^{-1}$).[25] These results suggest that the in situ generated Au NPs are catalytically active and that the NBs are accessible to reaction molecules in the outer solution through the ≈100 nm opening of the NBs.

In conclusion, silica NBs with a hydrophobic exterior surface and hydrophilic interior surface were synthesized by a one-pot sol–gel growth route. CPTMS plays key roles in controlling the NB shape and conferring moderate hydrophobic properties to the NB surface. Citrate-capped Pt NPs can be selectively loaded into the cavity of NBs by hydrogen bonding between the Pt NPs and the interior surface of the NBs. The Pt NPs@NB nanomotors can be self-propelled by the catalytic decomposition of H_2O_2, and exhibit a two-fold higher diffusion coefficient than nanomotors without the 3-chloropropyl groups capped on the exterior surface. Pilot studies reveal that the NBs can be efficiently used as nanovessels for diverse reactions, such as the in situ generation of Au NPs and catalytic reactions.

Experimental Section

Preparation of chemically asymmetric silica NBs: In a typical procedure, 3.0 g of PVP was dissolved in 30.0 mL of *n*-pentanol in a 50 mL centrifuge tube. 3.0 mL of ethanol and 1.68 mL of 0.2 M sodium citrate in ammonia aqueous solution were added, and the mixture was vigorously shaken. 300 μL of TBOS and 30 μL of CPTMS were then added to the above solution and shaken immediately for 5 min. The solution was left on a rotator (40 rpm) at room temperature (25 °C). After reaction for 2.5 h, the synthesized silica NBs were separated via centrifugation and washed twice with ethanol and water, respectively.

Acknowledgements

This work was financially supported by the National Natural Science Foundation of China (21373059, 21433002), National Key Basic Research Program of China (2013CB934101), the Australian Research Council (ARC) Centre of Excellence in Convergent Bio-Nano Science and Technology (project number CE140100036), and the ARC under the Australian Laureate Fellowship (F.C., FL120100030) scheme. Y.W. acknowledges support from the National 1000 Youth Talents Program of China.

Keywords: catalysis · hydrophobicity · nanomotor · nanoparticle · nanoreactor

How to cite: *Angew. Chem. Int. Ed.* **2016**, *55*, 14733–14737
Angew. Chem. **2016**, *128*, 14953–14957

[1] P. G. de Gennes, *Rev. Mod. Phys.* **1992**, *64*, 645–648.
[2] Y. Chen, H. Yang, C. Zhang, Q. Wang, X. Qu, J. Li, F. Liang, Z. Yang, *Macromolecules* **2013**, *46*, 4126–4130.
[3] S. Jiang, Q. Chen, M. Tripathy, E. Luijten, K. S. Schweizer, S. Granick, *Adv. Mater.* **2010**, *22*, 1060–1071.
[4] S. H. Kim, A. Abbaspourrad, D. A. Weitz, *J. Am. Chem. Soc.* **2011**, *133*, 5516–5524.
[5] a) G. A. Ozin, I. Manners, S. Fournier-Bidoz, A. Arsenault, *Adv. Mater.* **2005**, *17*, 3011–3018; b) X. Ma, K. Hahn, S. Sanchez, *J. Am. Chem. Soc.* **2015**, *137*, 4976–4979.
[6] a) F. Wang, G. M. Pauletti, J. Wang, J. Zhang, R. C. Ewing, Y. Wang, D. Shi, *Adv. Mater.* **2013**, *25*, 3485–3489; b) X. Li, L. Zhou, Y, Wei, A. M. EL-Toni, F. Zhang, D. Zhao, *J. Am. Chem. Soc.* **2014**, *136*, 15086–15092.
[7] S. H. Hu, X. Gao, *J. Am. Chem. Soc.* **2010**, *132*, 7234–7237.
[8] a) W. Gao, S. Sattayasamitsathit, J. Orozco, J. Wang, *J. Am. Chem. Soc.* **2011**, *133*, 11862–11864; b) S. Sánchez, L. Soler, J. Katuri, *Angew. Chem. Int. Ed.* **2015**, *54*, 1414–1444; *Angew. Chem.* **2015**, *127*, 1432–1464.
[9] M. Guix, C. C. Mayorga-Martinez, A. Merkoci, *Chem. Rev.* **2014**, *114*, 6285–6322.
[10] T. R. Kline, W. F. Paxton, T. E. Mallouk, A. Sen, *Angew. Chem. Int. Ed.* **2005**, *44*, 744–746; *Angew. Chem.* **2005**, *117*, 754–756.

[11] K. M. Manesh, M. Cardona, R. Yuan, M. Clark, D. Kagan, S. Balasubramanian, J. Wang, *ACS Nano* **2010**, *4*, 1799 – 1804.
[12] Y. Mei, G. Huang, A. A. Solovev, E. B. Urena, I. Moench, F. Ding, T. Reindl, R. K. Y. Fu, P. K. Chu, O. G. Schmidt, *Adv. Mater.* **2008**, *20*, 4085 – 4090.
[13] a) Y. P. He, J. S. Wu, Y. P. Zhao, *Nano Lett.* **2007**, *7*, 1369 – 1375; b) J. G. Gibbs, Y. P. Zhao, *Small* **2009**, *5*, 2304 – 2308.
[14] a) Y. Si, M. Chen, L. Wu, *Chem. Soc. Rev.* **2016**, *45*, 690 – 714; b) D. C. Hyun, P. Lu, S. I. Choi, U. Jeong, Y. Xia, *Angew. Chem. Int. Ed.* **2013**, *52*, 10468 – 10471; *Angew. Chem.* **2013**, *125*, 10662 – 10665; c) D. A. Wilson, R. J. M. Nolte, J. C. M. van Hest, *Nat. Chem.* **2012**, *4*, 268 – 274.
[15] D. Yi, C. Xu, R. Tang, X. Zhang, F. Caruso, Y. Wang, *Angew. Chem. Int. Ed.* **2016**, *55*, 8375 – 8380; *Angew. Chem.* **2016**, *128*, 8515 – 8520.
[16] A. Kuijk, A. van Blaaderen, A. Imhof, *J. Am. Chem. Soc.* **2011**, *133*, 2346 – 2349.
[17] a) Y. Boguslavsky, S. Margel, *J. Colloid Interface Sci.* **2008**, *317*, 101 – 114; b) T. Jesionowski, *Compos. Interfaces* **2009**, *16*, 115 – 129.
[18] Z. Zhang, C. Shao, P. Zou, P. Zhang, M. Zhang, J. Mu, Z. Guo, X. Li, C. Wang, Y. Liu, *Chem. Commun.* **2011**, *47*, 3906 – 3908.
[19] K. Sakakibara, J. P. Hill, K. Ariga, *Small* **2011**, *7*, 1288 – 1308.
[20] S. Sanchez, A. N. Ananth, V. M. Fomin, M. Viehrig, O. G. Schmidt, *J. Am. Chem. Soc.* **2011**, *133*, 14860 – 14863.
[21] G. Zhao, A. Ambrosi, M. Pumera, *Nanoscale* **2013**, *5*, 1319 – 1324.
[22] F. Shi, J. Niu, J. Liu, F. Liu, Z. Wang, X. Feng, X. Zhang, *Adv. Mater.* **2007**, *19*, 2257 – 2261.
[23] Y. Wang, R. M. Hernandez, D. J. Bartlett, J. M. Bingham, T. R. Kline, A. Sen, T. E. Mallouk, *Langmuir* **2006**, *22*, 10451 – 10456.
[24] a) R. Laocharoensuk, J. Burdick, J. Wang, *ACS Nano* **2008**, *2*, 1069 – 1075; b) U. K. Demirok, R. Laocharoensuk, K. M. Manesh, J. Wang, *Angew. Chem. Int. Ed.* **2008**, *47*, 9349 – 9351; *Angew. Chem.* **2008**, *120*, 9489 – 9491.
[25] a) E. Seo, J. Kim, Y. Hong, Y. S. Kim, D. Lee, B. S. Kim, *J. Phys. Chem. C* **2013**, *117*, 11686 – 11693; b) C. Xiao, S. Chen, L. Zhang, S. Zhou, W. Wu, *Chem. Commun.* **2012**, *48*, 11751 – 11753; c) J. Lee, J. C. Park, H. Song, *Adv. Mater.* **2008**, *20*, 1523 – 1528.

Received: July 28, 2016
Revised: September 8, 2016
Published online: October 20, 2016

